

1 Damaging missense variants in *IGF1R* implicate a role for IGF-1 resistance in the 2 aetiology of type 2 diabetes

3
4 Eugene J. Gardner^{@,1}, Katherine A. Kentistou¹, Stasa Stankovic¹, Samuel Lockhart², Eleanor
5 Wheeler¹, Felix R. Day¹, Nicola D. Kerrison¹, Nicholas J. Wareham¹, Claudia Langenberg^{1,4},
6 Stephen O'Rahilly^{*,2,3}, Ken K. Ong^{*,1,5}, John R. B. Perry^{*,@,1,6}

7
8 ¹MRC Epidemiology Unit, Wellcome–MRC Institute of Metabolic Science, University of Cambridge,
9 Cambridge, UK

10 ²MRC Metabolic Diseases Unit, Wellcome–MRC Institute of Metabolic Science, University of
11 Cambridge, Cambridge, UK

12 ³NIHR Cambridge Biomedical Research Centre, Cambridge, UK

13 ⁴Computational Medicine, Berlin Institute of Health at Charité–Universitätsmedizin Berlin, Berlin,
14 Germany

15 ⁵Department of Paediatrics, University of Cambridge, Cambridge, UK

16 ⁶Metabolic Research Laboratory, Wellcome–MRC Institute of Metabolic Science, University of
17 Cambridge, Cambridge, UK

18
19 * These authors jointly supervised this work

20 @ Corresponding authors: eugene.gardner@mrc-epid.cam.ac.uk; john.perry@mrc-epid.cam.ac.uk

22 Abstract

23 Type 2 diabetes (T2D) is a chronic metabolic disorder with a significant genetic component.
24 While large-scale population studies have identified hundreds of common genetic variants
25 associated with T2D susceptibility, the role of rare (minor allele frequency < 0.1%) protein
26 coding variation is less clear. To this end, we performed a gene burden analysis of 18,691
27 genes in 418,436 (n=32,374 T2D cases) individuals sequenced by the UK Biobank (UKBB)
28 study to assess the impact of rare genetic variants on T2D risk. Our analysis identified T2D
29 associations at exome-wide significance ($P < 6.9 \times 10^{-7}$) with rare, damaging variants within
30 previously identified genes including *GCK*, *GIGYF1*, *HNF1A*, and *TNRC6B*. In addition,
31 individuals with rare, damaging missense variants in the genes *ZEB2* (N=31 carriers;
32 OR=5.5 [95% CI=2.5-12.0]; $p=6.4 \times 10^{-7}$), *MLXIPL* (N=245; OR=2.3 [1.6-3.2]; $p=3.2 \times 10^{-7}$), and
33 *IGF1R* (N=394; OR=2.4 [1.8-3.2]; $p=1.3 \times 10^{-10}$) have higher risk of T2D. Carriers of damaging
34 missense variants within *IGF1R* were also shorter (-2.2cm [-1.8-2.7]; $p=1.2 \times 10^{-19}$) and had
35 higher circulating protein levels of insulin-like growth factor-1 (IGF-1; 2.3 nmol/L [1.7-2.9]
36 $p=2.8 \times 10^{-14}$), indicating relative IGF-1 resistance. A likely causal role of IGF-1 resistance on
37 T2D was further supported by Mendelian randomisation analyses using common variants.
38 Our results increase our understanding of the genetic architecture of T2D and highlight a
39 potential therapeutic benefit of targeting the Growth Hormone/IGF-1 axis.

40 Introduction

41 Type 2 diabetes (T2D) is a complex disease characterised by insulin resistance and beta-
42 cell dysfunction. An estimated 630 million adults are expected to have T2D by 2045¹ making
43 it one of the fastest growing global health challenges of the 21st century. Genome-wide

44 association studies (GWAS) have successfully identified more than 500 genomic loci to be
45 associated with T2D², although the majority of these are driven by common variants with
46 small individual effects on T2D risk.

47
48 Over 90% of GWAS loci lie in non-coding regions of the genome³, presenting a major hurdle
49 for the identification of the underlying causal genes and the translation of these findings into
50 mechanistic insight. In contrast, analysis of rare protein-coding variation captured by DNA
51 sequencing has the potential to more directly implicate individual genes and biological
52 mechanisms. The UK Biobank (UKBB)⁴ study recently made Exome Sequencing (ES) data
53 available for 454,787 UKBB participants⁵. This offers an unprecedented opportunity to
54 explore the contribution of rare coding variation to the risk of T2D with much greater power
55 than previously possible^{6–8}. Initial exome-wide association analyses of these data have
56 identified gene-based associations with increased risk of T2D for *GCK*, *HNF1A*, *HNF4A*,
57 *GIGYF1*, *CCAR2*, *TNRC6B* and *PAM*, and protective effects for variants in *FAM234A* and
58 *MAP3K15*^{5,9–14}.

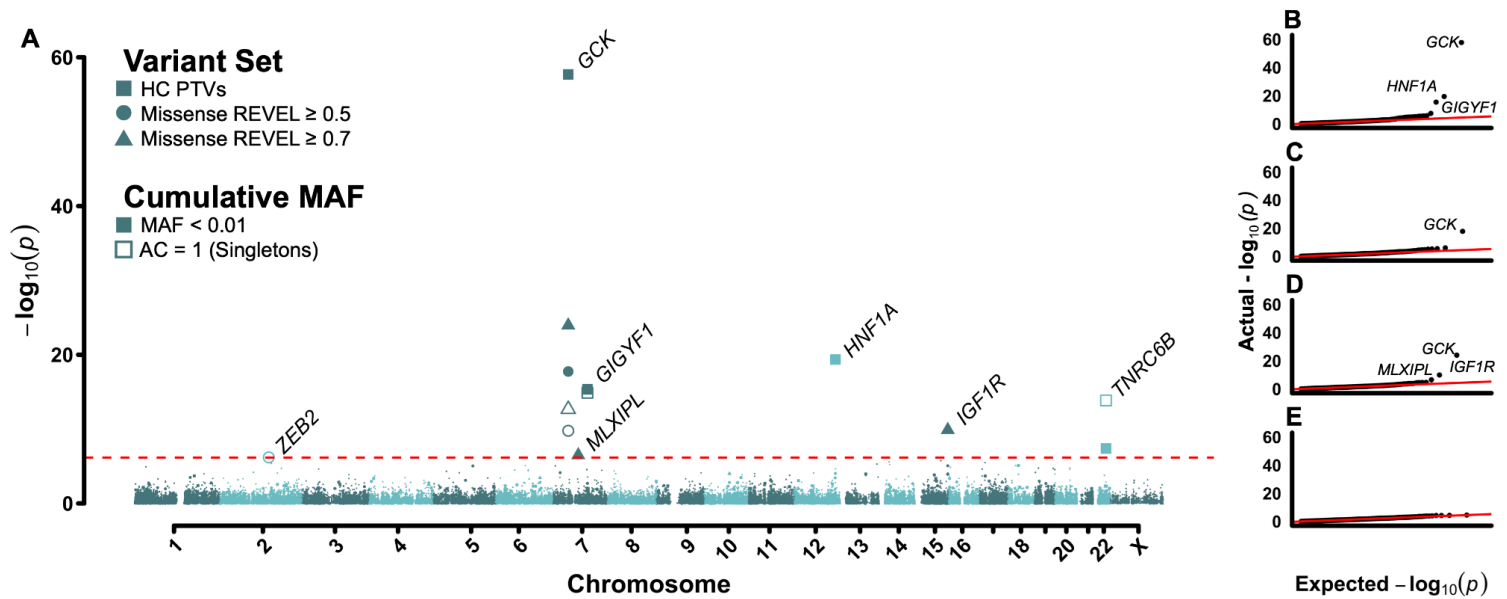
59
60 In this study, we combined multiple sources of health record data to identify additional T2D
61 cases and used an extended range of variant classes and allele frequency cutoffs in order to
62 directly implicate novel genes in the aetiology of T2D. Our results highlight a number of
63 previously missed associations and support a role for Insulin-like Growth Factor 1 (IGF-1)
64 resistance in the pathogenesis of T2D.

65 Results

66 Exome-wide burden testing in the UK Biobank

67 To identify genes associated with T2D risk, we performed an Exome-wide association study
68 (ExWAS) using ES data derived from 418,436 European genetic-ancestry UKBB
69 participants⁵. As our primary outcome, we identified 32,374 (7.7%) participants with likely
70 incident or prevalent T2D using phenotype curation that integrated multiple data sources,
71 including hospital episode statistics, self-reported conditions, death records, and use of T2D
72 medication (see methods).

73
74 Individual gene burden tests were performed by collapsing genetic variants across 18,691
75 protein-coding genes in the human genome. We tested four functional categories across two
76 population prevalences (minor allele frequency < 0.1% and singletons), including high-
77 confidence Protein Truncating Variants (PTVs), missense variants stratified by two REVEL
78 score thresholds¹⁵, and synonymous variants as a negative control (Figure 1; methods). We
79 identified 13 gene-functional annotation pairs with 30 or more rare allele carriers,
80 representing 7 non-redundant genes, associated with T2D at exome-wide statistical
81 significance ($p < 6.9 \times 10^{-7}$; Supplementary Table 1; methods). Our results are statistically
82 well-calibrated, both as indicated by low exome-wide inflation scores (e.g. PTV $\lambda=1.047$) and
83 by the absence of significant associations with synonymous variant burden (Figure 1B-E;
84 Supplementary Figure 1). To ensure our results were not biased by our approach, we
85 implemented burden tests using STAAR¹⁶ and a logistic model and arrived at substantially
86 similar conclusions (Supplementary Figure 2; Supplementary Table 1; methods).



88 **Figure 1. Exome-wide association results for T2D.** (A) Manhattan plot displaying results of gene
 89 burden tests for T2D risk. Genes passing exome-wide significance ($p < 6.9 \times 10^{-7}$) are labelled. Point
 90 shape indicates variant class tested. (B-E) QQ plots for (B) high confidence PTVs (C) REVEL ≥ 0.5
 91 Missense Variants (D) REVEL ≥ 0.7 missense variants and (E) synonymous variants (negative
 92 control).

93

94 We confirmed the T2D associations at all three genes identified by three previous studies of
 95 T2D risk that incorporated European genetic-ancestry individuals from the UKBB
 96 study^{11,12,14}: *GCK* (N=35 carriers; OR=58.5 [95% CI=25.5-134.5]; $p=2.0 \times 10^{-58}$), *HNF1A*
 97 (N=33; OR=12.7 [6.2-25.8]; $p=4.4 \times 10^{-20}$), and *GIGYF1* (N=133; OR=4.7 [3.1-7.0]; $p=4.4 \times 10^{-16}$;
 98 Figure 2). As in these previous studies, we similarly found that carriers of PTVs within
 99 these genes had substantially increased risk for developing T2D (Figure 1A).

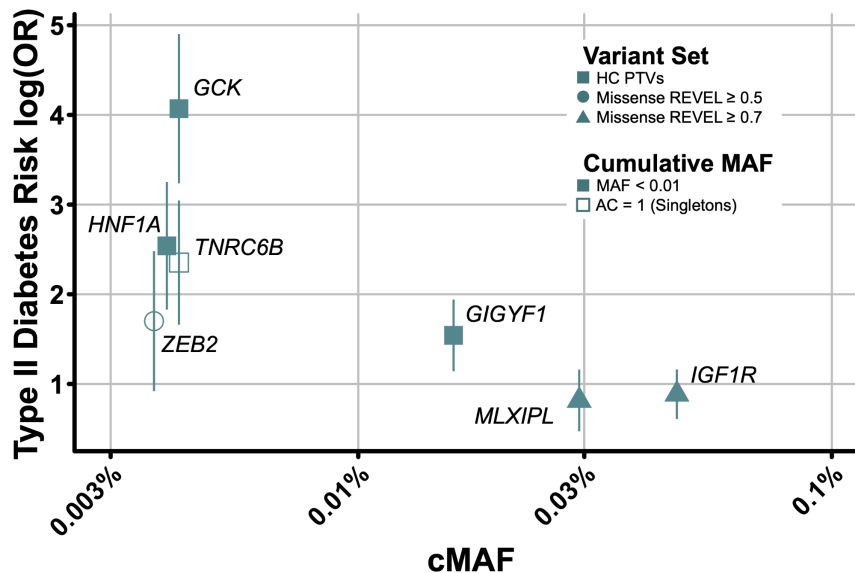
100

101 We also confirmed the T2D association at *TNRC6B* (N=35; OR=10.5 [5.3-21.0]; $p=1.4 \times 10^{-14}$),
 102 which was previously reported as 'potentially spuriously associated' with T2D risk¹¹;
 103 several new lines of evidence provide confidence in this association. Firstly, our result is not
 104 attributable to a single variant of large effect as evidenced by the strength of association with
 105 singleton variants (Figure 1A). Secondly, aside from a single individual carrying two
 106 balanced deletions, inspection of the underlying ES reads did not reveal a markedly
 107 increased error rate in variant calling or genotyping in *TNRC6B* as was suggested by Deaton
 108 et al.¹¹. Thirdly, the association persisted after excluding 14 individuals who carry a singleton
 109 PTV in a potentially non-constitutive exon as measured by PEXT ($p=3.6 \times 10^{-7}$)¹⁷. Finally, we
 110 also found that *TNRC6B* PTV carriers had elevated HbA1c levels when considering both
 111 T2D cases (4.1 mmol/mol [2.5-5.7]; $p=7.2 \times 10^{-7}$; Supplementary Figure 3) and controls (1.6
 112 mmol/mol [0.2-2.1]; $p=1.8 \times 10^{-2}$), consistent with the elevated long-term blood glucose levels
 113 observed in T2D patients.

114

115 We also identified three additional genes that, when disrupted by rare genetic variation
 116 (minor allele frequency $< 0.1\%$ or singletons), are associated with increased T2D risk:
 117 *IGF1R* (N=394; OR=2.4 [1.8-3.2]; $p=1.3 \times 10^{-10}$), *MLXIPL* (N=245; OR=2.3 [1.6-3.2];
 118 $p=3.2 \times 10^{-7}$), and *ZEB2* (N=31; OR=5.5 [2.5-12.0]; $p=6.4 \times 10^{-7}$; Figure 1). Unlike previously
 119 reported genes outlined above, damaging missense variants but not PTVs in these genes

120 were associated with T2D risk (Figure 2). Indeed, at these genes T2D associations were
121 apparent only with missense variants with high REVEL scores (≥ 0.7), or those variants
122 considered to be the most damaging as per current (2020) Association for Clinical Genomic
123 Science guidelines.
124



125
126 **Figure 2. Relationship between cumulative minor allele frequency and odds ratio for T2D.**
127 Plotted is T2D risk as quantified by log(Odds Ratio) versus cumulative minor allele frequencies
128 (cMAF) for genes significantly associated with T2D risk. For each gene, only the most significantly
129 associated variant mask is shown. Error bars indicate 95% confidence intervals.

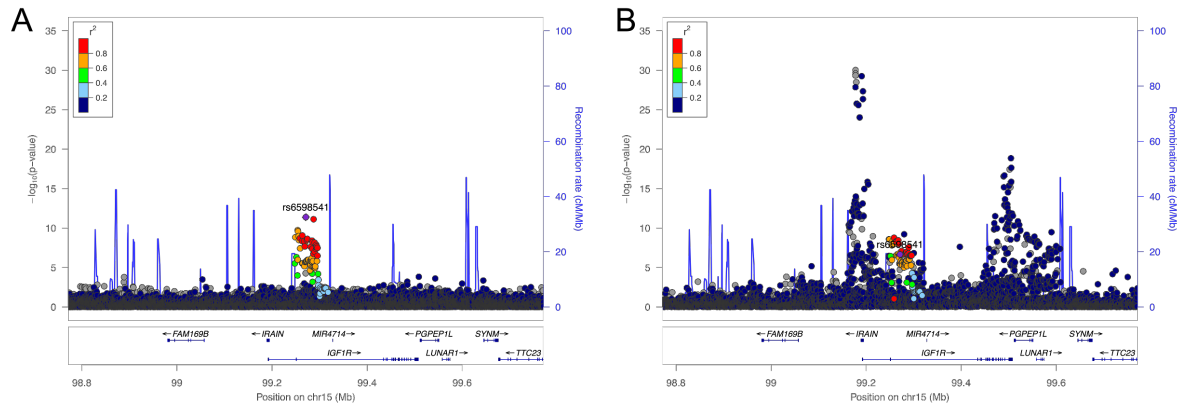
130
131 Specifically, and as expected, we found that carriers of PTVs within *GCK*, *GIGYF1*, and
132 *HNF1A* all had significantly elevated circulating glucose and HbA1c levels. Among novel
133 genes, *IGF1R* missense carriers had nominally higher HbA1c levels (1.1 mmol/mol [0.6-1.6];
134 $p=3.7 \times 10^{-6}$).

135 Exploring Common Variant Associations at Highlighted Genes

136 We next attempted to cross-validate the rare-variant associations for all seven exome-wide
137 significant genes by identifying proximal common variants (± 50 kb of a gene's coding
138 sequence) previously reported to be associated with related glycaemic or metabolic
139 phenotypes (methods; Supplementary Table 2). Four genes fell within glycaemic trait
140 associated loci and all seven overlapped known metabolic trait associations. For several of
141 these common variant-phenotype combinations, we also identified an association with rare
142 variant burden (Supplementary Figure 3). Additionally, three of the four novel genes we
143 report here were identified in the most recent publicly available T2D GWAS² as being either
144 the closest or most likely causal gene for a common variant genome-wide significant signal:
145 *IGF1R*, *TNRC6B*, and *ZEB2* (Supplementary Table 2).

146
147 Notably, common non-coding variants at the *IGF1R* locus have been previously reported for
148 T2D and fasting glucose^{2,18}. The lead fasting glucose-associated SNP (rs6598541-A; $p=$
149 4×10^{-12}) was associated with 0.0114 mmol/L [0.0097-0.0131] higher levels of glucose, while

150 the lead T2D SNP (rs59646751-T; $p=4\times 10^{-9}$) increases risk of T2D by an odds ratio of 1.024
151 [1.020-1.028]. Both SNPs are intronic in *IGF1R*, in moderate LD in European populations
152 ($R^2=75.5\%$)¹⁹, and are eQTLs for *IGF1R*²⁰. Furthermore, at both SNPs the *IGF1R*
153 expression-lowering alleles are associated with higher levels of circulating IGF-1 ($p=7\times 10^{-7}$
154 and 9×10^{-7} , respectively; Figure 3)²¹ and with higher T2D risk and fasting glucose.



155
156 **Figure 3. Common variant associations at the *IGF1R* locus.** Association pattern between SNPs at
157 the *IGF1R* locus and Fasting Glucose levels (A) and IGF-1 levels (B).

158 Interrogating *IGF1R* and Risk for T2D

159 To understand how rare damaging missense variants in *IGF1R* lead to increased risk of
160 T2D, we performed burden tests for circulating IGF-1 levels and anthropometric traits. We
161 found that carriers of damaging missense variants in *IGF1R* had increased circulating IGF-1
162 levels (2.1 nmol/L [1.5-2.6]; $p=1.9\times 10^{-14}$), but shorter adult stature (-2.2cm [-1.8-2.7];
163 $p=1.2\times 10^{-19}$), and lower relative height at age 10 ($p=1.1\times 10^{-7}$). These findings indicate that
164 carriers of rare damaging missense variants in *IGF1R* that increase risk of T2D have relative
165 IGF-1 resistance.

166
167 To explore how damaging missense variants disrupt *IGF1R* function, we next categorised
168 variants by protein domain. Carriers of qualifying variants within the *IGF1R* protein kinase
169 (residues 999-1274)²² had a higher risk for T2D (N= 179; OR=3.4 [2.3-4.9]; $p=1.9\times 10^{-10}$) than
170 those with qualifying variants outside this domain (N=215; OR=1.7 [1.2-2.6]; $p=8.2\times 10^{-3}$). We
171 thus conclude that dysfunction within the protein kinase domain could decrease downstream
172 signal transduction resulting in IGF-1 resistance. This may also explain why, despite the
173 relatively large number of *IGF1R* (N=64) PTV carriers in the UKBB, we did not find that
174 *IGF1R* PTV carriers had increased T2D risk. When bound by IGF-1 and to induce
175 downstream signal transduction, *IGF1R* functions as a homo or heterodimer (i.e. with *INSR*
176 as a hybrid receptor)²³. As half of a missense carrier's *IGF1R* molecules will contain errors in
177 the protein kinase domain, dimerisation will incorporate at least one defective molecule 75%
178 of the time and therefore lead to reduced downstream signal transduction. In the case of
179 PTV carriers, since one copy is likely missing due to nonsense-mediated decay, dimerisation
180 will always incorporate two functional copies. Therefore, the association of damaging *IGF1R*
181 missense variants with T2D may be due to a dominant-negative effect rather than decreased
182 protein abundance; however, additional functional studies are ultimately required to confirm
183 the mechanism underlying these variants.

184 To explore whether rare variants in other components of the GH-IGF1 hormone pathway
185 might influence T2D risk, we next identified a further nine genes in the GH-IGF1 pathway
186 that showed gene-burden associations with circulating IGF-1 levels in any of our burden
187 tests (Supplementary Table 3), including seven genes with known roles in regulating GH
188 secretion or GH signalling and three genes with known roles in IGF-1 bioavailability. We
189 tested their associations with childhood and adult height to indicate the functional relevance
190 of rare variation in these genes. None of the seven GH-related genes showed any
191 association with T2D. Rare damaging variants in *IGFALS*, which encodes a component of
192 the IGF-1 ternary complex, lowered lower circulating IGF-1 and were nominally associated
193 with shorter childhood height (indicative of lower IGF-1 bioactivity) and higher risk of T2D.
194 Rare damaging variants in *IGFBP3* (the major IGF binding protein), which lowered
195 circulating IGF-1 levels, were nominally associated with taller childhood height (indicative of
196 higher IGF-1 bioactivity) and lower risk of T2D. Hence damaging rare variants that disrupt
197 IGF-1 bioactivity, but not those that alter GH secretion or signalling, appear to increase T2D
198 risk.

199 Causality of IGF-1 Levels with T2D Risk

200 A previous epidemiological study described a protective association between baseline
201 circulating IGF-1 protein levels and incident T2D²⁴. However, subsequent similar studies
202 found no such association^{25,26} and conversely a previous study that modelled common
203 genetic variants in a Mendelian randomization framework inferred an adverse causal effect
204 of higher circulating IGF-1 levels on T2D²⁷.

205
206 To explore this apparent inconsistency, we examined the likely causal role of IGF-1 on T2D
207 by modelling 784 independent genetic signals for circulating IGF-1 levels identified in
208 428,525 white European UKBB individuals²¹ and summary statistics from the largest
209 reported GWAS meta-analysis of T2D²⁸. We confirmed the previously reported²⁷ association
210 between genetically-predicted higher IGF-1 levels and higher risk of T2D in inverse-variance
211 weighted (IVW; OR=1.105 per SD [95% CI 1.039-1.170]; $p=2.9 \times 10^{-3}$) and sensitivity models
212 (Supplementary Table 4). However, we noted substantial heterogeneity in the relationships
213 between individual IGF-1 signals and T2D (I-square=85.7%) as well as in their associations
214 with adult height (IVW Beta=0.142; $p=8.9 \times 10^{-9}$; I-square=97.7%). Among the common
215 genetic instruments for higher circulating IGF-1 levels, individual variants at the *IGF1* locus
216 (rs11111274) and the *IGF1R* locus (rs1815009) show directionally-opposite effects on
217 childhood height and T2D (taller height and lower T2D risk for IGF1; shorter height and
218 higher T2D risk for *IGF1R*; Supplementary Figure 4). Hence, reported common variant
219 instruments for higher IGF-1 levels comprise a mixture of functionally-opposing signals, i.e.
220 higher levels of bioactive IGF-1 but also higher IGF-1 resistance.

221 Discussion

222 Here we present the results of an ExWAS to assess the contribution of rare variant burden to
223 T2D risk (Figure 1). We identified three genes previously reported by a recent analysis of the
224 UKBB (*GCK*, *HNF1A*, and *GIGYF1*)¹⁴, provide stronger evidence for a previously nominally
225 associated gene (*TNRC6B*)¹¹, and identified three new genes (*ZEB2*, *MLXIPL*, and *IGF1R*)
226 where rare variants increase susceptibility to T2D (Figure 2). Using publicly available data,

227 we showed that common variation nearby these genes is associated with a wide range of
228 glycemic and metabolic traits and (Figure 3; Supplementary Table 2)^{2,18}, providing further
229 support for these rare variant associations. We further interrogated rare and common variant
230 associations to show that disruption of *IGF1R* due to damaging missense variants in the
231 cytoplasmic protein kinase domain leads to IGF-1 resistance and higher T2D risk. Overall,
232 our results implicate a wider protective effect of IGF-1 bioactivity on susceptibility to T2D.

233 While our results are complementary to previous ExWAS^{11,14}, we clarified evidence linking
234 *TNRC6B* to T2D and identified three additional genes missed by previous analyses of the
235 UKBB. A key advantage of our approach was to carefully curate multiple data sources to
236 identify and validate T2D cases. Furthermore, we used a different genetic analytical
237 approach to those previous studies. Nag et al.¹⁴ limited their burden testing to either PTVs,
238 the findings of which we replicate here, or to missense variants with comparatively low
239 deleteriousness scores (REVEL > 0.25 or Missense Tolerance Ratio intragenic percentiles ≤
240 50%). In this study, we have shown the benefit of considering missense variants
241 computationally predicted to be severely damaging (REVEL ≥ 0.5 and 0.7)¹⁵. While such
242 variants are much rarer in the population – only ~8% of missense variants in UKBB have
243 REVEL scores ≥ 0.7 – they are much more likely to disrupt protein function and thus
244 increase risk for disease. These conclusions are similar to those shown previously for
245 anthropometric traits¹⁰, which have shown a relationship between PTVs in *IGF1R* and
246 several growth measures, but not for damaging missense variants.

247 A key finding of our work is the novel association between *IGF1R* and T2D risk. Loss of
248 function mutations in *IGF1R* have been reported in children presenting with intra-uterine
249 growth restriction, short stature and elevated IGF-1 levels²⁹⁻³¹. Our findings of rare damaging
250 variants at *IGF1R*, and also at *IGFALS* and *IGFBP3*, indicate that reduced IGF-1 bioactivity
251 and signalling increases risk for T2D. There are several plausible mechanisms to link *IGF1R*
252 to T2D. *IGF1R*, responding to both systemic and locally generated IGF-1, may play a role in
253 the development of several tissues central to the control of glucose metabolism including
254 pancreatic islets, adipose tissue and skeletal muscle³². An alternative explanation involves
255 the complex relationship between growth hormone (GH) and IGF-1. GH, produced in a
256 highly controlled and pulsatile manner from the somatotropes of the anterior pituitary, is the
257 major stimulus to the hepatic expression and secretion of IGF-1, the major source of this
258 circulating hormone. GH also has metabolic effects that are independent of IGF-1, largely
259 exerted by its powerful lipolytic effects in adipose tissue³³⁻³⁸, which if uncontrolled can lead
260 to the accumulation of ectopic lipid in non-adipose tissue resulting in insulin resistance. This
261 is elegantly demonstrated by studies in mice in which IGF-1 is selectively deleted in the
262 liver^{39,40}. These mice show a striking increase in circulating GH levels, accompanied by
263 marked insulin resistance which is entirely abrogated by the blockade of GH signalling. This
264 model can explain the insulin resistance and frequent T2D seen in conditions such as
265 acromegaly, where GH and IGF-1 levels are persistently raised due to a functional
266 somatotrope tumour⁴¹, and the striking protection from T2D seen in patients with Laron
267 Dwarfism, whose markedly reduced circulating IGF-1 levels are due to biallelic LoF
268 mutations in the GH receptor⁴². Loss of function mutations in *IGF1R* are likely to result in
269 compensatory increases in GH secretion, and consequently higher levels of circulating IGF-1
270 that we observed in the carriers of such mutations. While this may partially compensate for
271 impairment in *IGF1R* function, the *IGF1R*-independent effects of GH are likely to have a
272 deleterious effect on systemic glucose metabolism. Of note in this regard, a single human
273 proband with a homozygous loss of function mutation in *IGF-1* had elevated circulating GH
274 and severe insulin resistance^{43,44}. Therapy with exogenous IGF-1 resulted in suppression of

275 GH and a dose dependent improvement in insulin sensitivity⁴⁴. Accordingly, genetically
276 reduced GH secretion and signalling would lead to reduced IGF-1 bioactivity, but without the
277 consequent effects of elevated GH on fatty acid metabolism and insulin resistance, and
278 hence no alteration in T2D risk. We propose that currently available drugs which reduce GH
279 secretion or block its action may have metabolic benefits in patients with T2D and damaging
280 missense variants in the protein kinase domain of *IGF1R*.

281
282 Our findings also demonstrate the challenge of interpreting Mendelian randomisation results
283 of circulating biomarkers. Elevated levels may reflect higher levels of secretion and
284 biomarker activity, but are also increased by mechanisms that reduce biomarker
285 bioavailability or sensitivity. Hence, genetic instruments for higher biomarker levels may
286 comprise a mixture of markers for both higher and lower biomarker activity. To distinguish
287 these actions, we suggest that individual common variants are first tested for association
288 with some indicator of biomarker activity (i.e. childhood height as an indicator of IGF-1
289 activity).

290
291 Our rare variant analysis also implicates *MLXIPL* as a T2D susceptibility gene for the first
292 time. *MLXIPL* encodes the carbohydrate response element binding protein (CHREBP), a
293 transcription factor that acts in concert with its obligate binding partner MLX to regulate the
294 cellular response to carbohydrate⁴⁵⁻⁴⁷ and is highly expressed in liver, fat, and muscle.
295 Global or tissue-specific ablation of *MLXIPL* in mice impairs insulin sensitivity⁴⁸⁻⁵¹. Common
296 variants at the *MLXIPL* locus associate with *SHBG*, a biomarker of insulin sensitivity⁵² and
297 with serum triglycerides^{53,54}. Notably, *MLXIPL* is one of the 26-28 genes deleted in Williams
298 Syndrome, the result of a deletion of contiguous genes on chromosome 7q11.23. Patients
299 with this syndrome are characterised by marked insulin resistance and an increased risk of
300 diabetes⁵⁵. It seems likely that haploinsufficiency⁵⁵ for *MLXIPL* contributes significantly to the
301 metabolic disturbances characteristic of Williams syndrome.

302
303 Overall, our findings suggest that deeper interrogation of multiple variant types when
304 performing ExWAS can and will lead to the discovery of additional genes associated with a
305 wide-range of human diseases.

306 Methods

307 UK Biobank Data Processing and Quality Control

308 To conduct rare variant burden analyses outlined in this publication, we queried ES data for
309 454,787 individuals provided by the UKBB study⁵. Individuals were excluded from further
310 analysis if they had excess heterozygosity, autosomal variant missingness on genotyping
311 arrays $\geq 5\%$, or were not included in the subset of phased samples as defined in Bycroft et
312 al.⁵⁶. We further excluded all study participants who were not of broadly European genetic
313 ancestry, leaving a total of 421,065 individuals for further analysis.

314
315 To perform variant quality control and annotation, we utilised the UKBB Research Analysis
316 Platform (RAP; <https://ukbiobank.dnanexus.com/>). The RAP is a cloud-based compute
317 environment which provides a central data repository for UKBB ES and phenotypic data.

318 Using bespoke applets designed for the RAP, we performed additional quality control of ES
319 data beyond that already documented in Backman et al.⁵. Using provided population-level
320 Variant Call Format (VCF) files, we first split and left-corrected multi-allelic variants into
321 separate alleles using 'bcftools norm'⁵⁷. Next, we performed genotype-level filtering using
322 'bcftools filter' separately for Single Nucleotide Variants (SNVs) and Insertions/Deletions
323 (InDels) using a missingness-based approach. With this approach, SNV genotypes with
324 depth < 7 and genotype quality < 20 or InDel genotypes with a depth < 10 and genotype
325 quality < 20 were set to missing (i.e. '.'). We further tested for an expected alternate allele
326 contribution of 50% for heterozygous SNVs using a binomial test; SNV genotypes with a
327 binomial test p. value $\leq 1 \times 10^{-3}$ were set to missing. Following genotype-level filtering we
328 recalculated the proportion of individuals with a missing genotype for each variant and
329 filtered all variants with a missingness value > 50%.

330
331 We next annotated variants using the ENSEMBL Variant Effect Predictor (VEP) v104⁵⁸ with
332 the '--everything' flag and plugins for REVEL¹⁵, CADD⁵⁹, and LOFTEE⁶⁰ enabled. For each
333 variant, we prioritised a single ENSEMBL transcript based on whether or not the annotated
334 transcript was protein-coding, MANE select v0.97, or the VEP Canonical transcript,
335 respectively. Individual consequence for each variant was prioritised based on severity as
336 defined by VEP. Following annotation, we grouped stop gained, frameshift, splice acceptor,
337 and splice donor variants into a single Protein Truncating Variant (PTV) category. Missense
338 and synonymous variant consequences are identical to those defined by VEP. Only
339 autosomal or chrX variants within ENSEMBL protein-coding transcripts and within transcripts
340 included on the UKBB ES assay were retained for subsequent burden testing.

341 Exome-wide association analyses in the UK Biobank

342 To perform rare variant burden tests using filtered and annotated ES data, we employed a
343 custom implementation of BOLT-LMM v2.3.6⁶¹ for the RAP. BOLT-LMM expects two primary
344 inputs: i) a set of genotypes with minor allele count > 100 derived from genotyping arrays to
345 construct a null model and ii) a larger set of imputed variants to perform association tests.
346 For the former, we queried genotyping data available on the RAP and restricted to an
347 identical set of individuals used for rare variant association tests. For the latter, and as
348 BOLT-LMM expects imputed genotyping data as input rather than per-gene carrier status,
349 we created dummy genotype files where each variant represents one gene and individuals
350 with a qualifying variant within that gene are coded as heterozygous, regardless of the
351 number of variants that individual has in that gene. To test a range of variant annotation
352 categories across the allele frequency spectrum, we created dummy genotype files for minor
353 allele frequency < 0.1% and singleton high confidence PTVs as defined by LOFTEE,
354 missense variants with REVEL ≥ 0.5 , missense variants with REVEL ≥ 0.7 , and synonymous
355 variants. For each phenotype tested, BOLT-LMM was then run with default parameters other
356 than the inclusion of the 'ImmInfOnly' flag. When exploring the role of rare variants in the
357 IGF-1/GH axis and to incorporate less deleterious missense variants, we also used an
358 additional set of variant annotations which combined missense variants with CADD ≥ 25 and
359 high confidence PTVs (i.e. Damaging; Supplementary Table 3). To derive association
360 statistics for individual variants, we also provided all 26,657,229 individual markers
361 regardless of filtering status as input to BOLT-LMM. All tested phenotypes were run as
362 continuous traits corrected by age, age², sex, the first ten genetic principal components as

363 calculated in Bycroft et al.⁵⁶, and study participant ES batch as a categorical covariate (either
364 50k, 200k, or 450k). For phenotype definitions used in this study, please refer to
365 Supplementary Table 5. Only the first instance (initial visit) was used for generating all
366 phenotype definitions unless specifically noted in Supplementary Table 5.

367

368 To provide an orthogonal approach to validate our BOLT-LMM results, we also performed
369 per-gene burden tests with STAAR¹⁶ and a generalised linear model as implemented in the
370 python package 'statsmodels'⁶². To run STAAR, we created a custom Python and R
371 workflow on the RAP. VCF files were first converted into a sparse matrix suitable for use with
372 the R package 'Matrix' using 'bcftools query'. Using the 'STAAR' R package, we first ran a
373 null model with identical coefficients to BOLT-LMM and a sparse relatedness matrix with a
374 relatedness coefficient cutoff of 0.125 as described by Bycroft et al.⁵⁶. We next used the
375 function 'STAAR' to test all protein-coding transcripts as outlined above. To run generalised
376 linear models, we used a three step process. First, we ran a null model with all dependent
377 variables as continuous traits, corrected for control covariates identical to those included in
378 BOLT-LMM. Next, using the residuals of this null model, we performed initial regressions on
379 carrier status to obtain a preliminary p. value. Finally, for individual genes that passed a
380 lenient p. value threshold of $<1 \times 10^{-4}$, we recalculated a full model to obtain exact test
381 statistics with family set to 'binomial' or 'gaussian' if the trait was binary or continuous,
382 respectively. Generalised linear models utilised identical input to BOLT-LMM converted to a
383 sparse matrix.

384 Common variant GWAS lookups

385 Common variant associations at the identified genes were queried using the T2D Knowledge
386 Portal (<https://t2d.hugeamp.org>) and the Open Targets Genetics platform
387 (<https://genetics.opentargets.org/>)⁶³. Trait associations from the T2D Knowledge Portal are
388 presented in Supplementary Table 2 and were only included if the paired gene was assigned
389 as the nearest gene to the association signal as a crude proxy for causality. Accompanying
390 HuGE scores were extracted for the highest-scoring glycaemic common variants
391 associations. Locus2Gene scores based on data from Vujkovic et al.² were extracted from
392 the Open Targets Genetics platform and are presented in Supplementary Table 2. For the
393 *IGF1R* locus follow-up, we used sentinel SNP information for Vujkovic et al.² and summary
394 statistics from the recent fasting glucose MAGIC meta-analysis¹⁸ and circulating IGF-1 levels
395 GWAS. eQTL data was accessed through GTEx v8²⁰. Effect estimates in the text have been
396 aligned towards the T2D/glucose increasing alleles, using LD information from LDlink¹⁹.
397 Regions in Figure 3 were plotted using LocusZoom⁶⁴.

398 Mendelian Randomisation Using IGF-1 levels

399 To examine the likelihood of a causal effect of IGF-1 on the risk of T2D, we applied
400 Mendelian randomization (MR) analysis. In this approach, genetic variants that are
401 significantly associated with an exposure of interest are used as instrumental variables (IVs)
402 to test the causality of that exposure on the outcome of interest. For a genetic variant to be a
403 reliable instrument, the following assumptions should be met: (1) the genetic instrument is
404 associated with the exposure of interest, (2) the genetic instrument should not be associated
405 with any other competing risk factor that is a confounder, and (3) the genetic instrument

406 should not be associated with the outcome, except via the causal pathway that includes the
407 exposure of interest⁶⁵. As IVs, we used the 831 IGF-1 genome-wide significant signals
408 reported in a recent GWAS on IGF-1²¹. As our outcome data, we selected the largest
409 publicly available independent T2D dataset available in 893,130 European genetic ancestry
410 individuals (9% cases) from Mahajan et al.²⁸ If a signal was not present in the outcome
411 GWAS, we searched the UKBB white European dataset for proxies (within 1 Mb and $r^2 >$
412 0.5) and chose the variant with the highest r^2 value, which left 784 independent markers for
413 MR analysis. Genotypes at all variants were aligned to designate the IGF-1-increasing
414 alleles as the effect alleles.

415
416 To conduct our MR analysis, we used the inverse-variance weighted (IVW) model as the
417 primary model as it offers the most statistical power⁶⁶; however, as it does not correct for
418 heterogeneity in outcome risk estimates between individual variants⁶⁷, we applied a number
419 of sensitivity MR methods that better account for heterogeneity⁶⁸. These include an Egger
420 analysis to identify and correct for unbalanced heterogeneity ('horizontal pleiotropy'),
421 indicated by a significant Egger intercept ($p < 0.05$)⁶⁹, and weighted median (WM) and
422 penalised weighted median (PWM) models to correct for balanced heterogeneity⁷⁰. In
423 addition, we introduced the radial method to exclude variants from each model in cases
424 where they are recognized as outliers, as well as Steiger filtering to assess for potential
425 reverse causality (i.e. variants with stronger association with the outcome than with the
426 exposure)⁷¹. As previous work on IGF-1 showed a strong association with height, and to a
427 lesser extent BMI²⁷, we also used multivariable MR analysis⁷² to estimate the direct effect of
428 IGF-1 levels on T2D not mediated by BMI or height by adjusting for their effects as
429 covariates using queried phenotype data for UKBB participants (Supplementary Table 4;
430 Supplementary Table 5). In order to examine the individual level effect of IGF1 and IGF1R
431 loci on T2D, BMI, childhood and adult height, we performed the variant-specific lookups as
432 well as calculated the Wald ratio using the R package 'TwoSampleMR'⁷³. All results
433 presented in the main text are expressed in standard deviations of IGF-1 levels (one S.D. is
434 equivalent to ~5.5 nmol/L in UKBB). Values available in Supplementary Table 4 are raw
435 data, per unit IGF-1.

436 Acknowledgements

437 This work was funded by the Medical Research Council (Unit programs: MC_UU_12015/2,
438 MC_UU_00006/2, MC_UU_12015/1, and MC_UU_00006/1). S.L. is supported by a
439 Wellcome Trust Clinical PhD Fellowship (225479/Z/22/Z). This research was supported by
440 the NIHR Cambridge Biomedical Research Centre (BRC-1215-20014). For the purpose of
441 open access, the author has applied a Creative Commons Attribution (CC BY) licence to any
442 Author Accepted Manuscript version arising. This research was conducted using the UK
443 Biobank Resource under application 9905.

444 References

- 445 1. International Diabetes Federation. *IDF Diabetes Atlas, 9th Edition*. (International
446 Diabetes Federation, 2021).

- 447 2. Vujkovic, M. *et al.* Discovery of 318 new risk loci for type 2 diabetes and related
448 vascular outcomes among 1.4 million participants in a multi-ancestry meta-analysis.
449 *Nat. Genet.* **52**, 680–691 (2020).
- 450 3. Loos, R. J. F. 15 years of genome-wide association studies and no signs of slowing
451 down. *Nat. Commun.* **11**, 5900 (2020).
- 452 4. Szustakowski, J. D. *et al.* Advancing human genetics research and drug discovery
453 through exome sequencing of the UK Biobank. *Nat. Genet.* **53**, 942–948 (2021).
- 454 5. Backman, J. D. *et al.* Exome sequencing and analysis of 454,787 UK Biobank
455 participants. *Nature* **599**, 628–634 (2021).
- 456 6. Fuchsberger, C. *et al.* The genetic architecture of type 2 diabetes. *Nature* **536**, 41–47
457 (2016).
- 458 7. Flannick, J. *et al.* Exome sequencing of 20,791 cases of type 2 diabetes and 24,440
459 controls. *Nature* **570**, 71–76 (2019).
- 460 8. Langenberg, C. & Lotta, L. A. Genomic insights into the causes of type 2 diabetes.
461 *Lancet* **391**, 2463–2474 (2018).
- 462 9. Curtis, D. Analysis of rare coding variants in 200,000 exome-sequenced subjects
463 reveals novel genetic risk factors for type 2 diabetes. *Diabetes. Metab. Res. Rev.* **38**,
464 e3482 (2022).
- 465 10. Wang, Q. *et al.* Rare variant contribution to human disease in 281,104 UK Biobank
466 exomes. *Nature* **597**, 527–532 (2021).
- 467 11. Deaton, A. M. *et al.* Gene-level analysis of rare variants in 379,066 whole exome
468 sequences identifies an association of GIGYF1 loss of function with type 2 diabetes.
469 *Sci. Rep.* **11**, 21565 (2021).
- 470 12. Zhao, Y. *et al.* GIGYF1 loss of function is associated with clonal mosaicism and adverse
471 metabolic health. *Nat. Commun.* **12**, 4178 (2021).
- 472 13. Jurgens, S. J. *et al.* Analysis of rare genetic variation underlying cardiometabolic
473 diseases and traits among 200,000 individuals in the UK Biobank. *Nat. Genet.* (2022)
474 doi:10.1038/s41588-021-01011-w.

- 475 14. Nag, A. *et al.* Human genetic evidence supports MAP3K15 inhibition as a therapeutic
476 strategy for diabetes. *Cold Spring Harbor Laboratory* (2021)
477 doi:10.1101/2021.11.14.21266328.
- 478 15. Ioannidis, N. M. *et al.* REVEL: An Ensemble Method for Predicting the Pathogenicity of
479 Rare Missense Variants. *Am. J. Hum. Genet.* **99**, 877–885 (2016).
- 480 16. Li, X. *et al.* Dynamic incorporation of multiple in silico functional annotations empowers
481 rare variant association analysis of large whole-genome sequencing studies at scale.
482 *Nat. Genet.* **52**, 969–983 (2020).
- 483 17. Cummings, B. B. *et al.* Transcript expression-aware annotation improves rare variant
484 interpretation. *Nature* **581**, 452–458 (2020).
- 485 18. Chen, J. *et al.* The trans-ancestral genomic architecture of glycemic traits. *Nat. Genet.*
486 **53**, 840–860 (2021).
- 487 19. Machiela, M. J. & Chanock, S. J. LDlink: a web-based application for exploring
488 population-specific haplotype structure and linking correlated alleles of possible
489 functional variants. *Bioinformatics* **31**, 3555–3557 (2015).
- 490 20. GTEx Consortium. The GTEx Consortium atlas of genetic regulatory effects across
491 human tissues. *Science* **369**, 1318–1330 (2020).
- 492 21. Stankovic, S. *et al.* Elucidating the genetic architecture underlying IGF1 levels and its
493 impact on genomic instability and cancer risk. *Wellcome Open Research* (2021)
494 doi:10.12688/wellcomeopenres.16417.1.
- 495 22. Favelyukis, S., Till, J. H., Hubbard, S. R. & Miller, W. T. Structure and autoregulation of
496 the insulin-like growth factor 1 receptor kinase. *Nat. Struct. Biol.* **8**, 1058–1063 (2001).
- 497 23. Li, J., Choi, E., Yu, H. & Bai, X.-C. Structural basis of the activation of type 1 insulin-like
498 growth factor receptor. *Nat. Commun.* **10**, 4567 (2019).
- 499 24. Sandhu, M. S. *et al.* Circulating concentrations of insulin-like growth factor-I and
500 development of glucose intolerance: a prospective observational study. *Lancet* **359**,
501 1740–1745 (2002).
- 502 25. Lewitt, M. S. *et al.* IGF-binding protein 1 and abdominal obesity in the development of

- 503 type 2 diabetes in women. *Eur. J. Endocrinol.* **163**, 233–242 (2010).
- 504 26. Similä, M. E. *et al.* Insulin-like growth factor I, binding proteins -1 and -3, risk of type 2
505 diabetes and macronutrient intakes in men. *Br. J. Nutr.* **121**, 938–944 (2019).
- 506 27. Larsson, S. C., Michaëlsson, K. & Burgess, S. IGF-1 and cardiometabolic diseases: a
507 Mendelian randomisation study. *Diabetologia* **63**, 1775–1782 (2020).
- 508 28. Mahajan, A. *et al.* Fine-mapping type 2 diabetes loci to single-variant resolution using
509 high-density imputation and islet-specific epigenome maps. *Nat. Genet.* **50**, 1505–1513
510 (2018).
- 511 29. Abuzzahab, M. J. *et al.* IGF-I receptor mutations resulting in intrauterine and postnatal
512 growth retardation. *N. Engl. J. Med.* **349**, 2211–2222 (2003).
- 513 30. Fang, P. *et al.* Severe short stature caused by novel compound heterozygous mutations
514 of the insulin-like growth factor 1 receptor (IGF1R). *J. Clin. Endocrinol. Metab.* **97**,
515 E243–7 (2012).
- 516 31. Inagaki, K. *et al.* A familial insulin-like growth factor-I receptor mutant leads to short
517 stature: clinical and biochemical characterization. *J. Clin. Endocrinol. Metab.* **92**, 1542–
518 1548 (2007).
- 519 32. Rother, K. I. & Accili, D. Role of insulin receptors and IGF receptors in growth and
520 development. *Pediatr. Nephrol.* **14**, 558–561 (2000).
- 521 33. Kopchick, J. J., Berryman, D. E., Puri, V., Lee, K. Y. & Jorgensen, J. O. L. The effects of
522 growth hormone on adipose tissue: old observations, new mechanisms. *Nat. Rev.*
523 *Endocrinol.* **16**, 135–146 (2020).
- 524 34. Arlien-Søborg, M. C. *et al.* Reversible insulin resistance in muscle and fat unrelated to
525 the metabolic syndrome in patients with acromegaly. *EBioMedicine* **75**, 103763 (2022).
- 526 35. Nielsen, S., Møller, N., Christiansen, J. S. & Jørgensen, J. O. Pharmacological
527 antilipolysis restores insulin sensitivity during growth hormone exposure. *Diabetes* **50**,
528 2301–2308 (2001).
- 529 36. Høyer, K. L. *et al.* The acute effects of growth hormone in adipose tissue is associated
530 with suppression of antilipolytic signals. *Physiol Rep* **8**, e14373 (2020).

- 531 37. Møller, N. *et al.* Effects of a growth hormone pulse on total and forearm substrate fluxes
532 in humans. *Am. J. Physiol.* **258**, E86–91 (1990).
- 533 38. Ran, L. *et al.* Loss of Adipose Growth Hormone Receptor in Mice Enhances Local Fatty
534 Acid Trapping and Impairs Brown Adipose Tissue Thermogenesis. *iScience* **16**, 106–
535 121 (2019).
- 536 39. Yakar, S. *et al.* Inhibition of growth hormone action improves insulin sensitivity in liver
537 IGF-1-deficient mice. *J. Clin. Invest.* **113**, 96–105 (2004).
- 538 40. Yakar, S. *et al.* Liver-specific igf-1 gene deletion leads to muscle insulin insensitivity.
539 *Diabetes* **50**, 1110–1118 (2001).
- 540 41. Mestron, A. *et al.* Epidemiology, clinical characteristics, outcome, morbidity and
541 mortality in acromegaly based on the Spanish Acromegaly Registry (Registro Espanol
542 de Acromegalia, REA). *Eur. J. Endocrinol.* **151**, 439–446 (2004).
- 543 42. Guevara-Aguirre, J. *et al.* Growth hormone receptor deficiency is associated with a
544 major reduction in pro-aging signaling, cancer, and diabetes in humans. *Sci. Transl.*
545 *Med.* **3**, 70ra13 (2011).
- 546 43. Woods, K. A., Camacho-Hübner, C., Savage, M. O. & Clark, A. J. Intrauterine growth
547 retardation and postnatal growth failure associated with deletion of the insulin-like
548 growth factor I gene. *N. Engl. J. Med.* **335**, 1363–1367 (1996).
- 549 44. Woods, K. A. *et al.* Effects of insulin-like growth factor I (IGF-I) therapy on body
550 composition and insulin resistance in IGF-I gene deletion. *J. Clin. Endocrinol. Metab.* **85**,
551 1407–1411 (2000).
- 552 45. Yamashita, H. *et al.* A glucose-responsive transcription factor that regulates
553 carbohydrate metabolism in the liver. *Proc. Natl. Acad. Sci. U. S. A.* **98**, 9116–9121
554 (2001).
- 555 46. Ma, L., Tsatsos, N. G. & Towle, H. C. Direct role of ChREBP.Mlx in regulating hepatic
556 glucose-responsive genes. *J. Biol. Chem.* **280**, 12019–12027 (2005).
- 557 47. Stoeckman, A. K., Ma, L. & Towle, H. C. Mlx is the functional heteromeric partner of the
558 carbohydrate response element-binding protein in glucose regulation of lipogenic

- 559 enzyme genes. *J. Biol. Chem.* **279**, 15662–15669 (2004).
- 560 48. Abdul-Wahed, A., Guilmeau, S. & Postic, C. Sweet Sixteenth for ChREBP: Established
561 Roles and Future Goals. *Cell Metab.* **26**, 324–341 (2017).
- 562 49. Jois, T. *et al.* Deletion of hepatic carbohydrate response element binding protein
563 (ChREBP) impairs glucose homeostasis and hepatic insulin sensitivity in mice. *Mol*
564 *Metab* **6**, 1381–1394 (2017).
- 565 50. Vijayakumar, A. *et al.* Absence of Carbohydrate Response Element Binding Protein in
566 Adipocytes Causes Systemic Insulin Resistance and Impairs Glucose Transport. *Cell*
567 *Rep.* **21**, 1021–1035 (2017).
- 568 51. Iizuka, K., Bruick, R. K., Liang, G., Horton, J. D. & Uyeda, K. Deficiency of carbohydrate
569 response element-binding protein (ChREBP) reduces lipogenesis as well as glycolysis.
570 *Proc. Natl. Acad. Sci. U. S. A.* **101**, 7281–7286 (2004).
- 571 52. Ruth, K. S. *et al.* Using human genetics to understand the disease impacts of
572 testosterone in men and women. *Nat. Med.* **26**, 252–258 (2020).
- 573 53. Kanai, M. *et al.* Genetic analysis of quantitative traits in the Japanese population links
574 cell types to complex human diseases. *Nat. Genet.* **50**, 390–400 (2018).
- 575 54. Klarin, D. *et al.* Genetics of blood lipids among ~300,000 multi-ethnic participants of the
576 Million Veteran Program. *Nat. Genet.* **50**, 1514–1523 (2018).
- 577 55. Stagi, S. *et al.* Williams-beuren syndrome is a genetic disorder associated with impaired
578 glucose tolerance and diabetes in childhood and adolescence: new insights from a
579 longitudinal study. *Horm. Res. Paediatr.* **82**, 38–43 (2014).
- 580 56. Bycroft, C. *et al.* The UK Biobank resource with deep phenotyping and genomic data.
581 *Nature* **562**, 203–209 (2018).
- 582 57. Danecek, P. *et al.* Twelve years of SAMtools and BCFtools. *Gigascience* **10**, (2021).
- 583 58. McLaren, W. *et al.* The Ensembl Variant Effect Predictor. *Genome Biol.* **17**, 122 (2016).
- 584 59. Rentzsch, P., Witten, D., Cooper, G. M., Shendure, J. & Kircher, M. CADD: predicting
585 the deleteriousness of variants throughout the human genome. *Nucleic Acids Res.* **47**,
586 D886–D894 (2019).

- 587 60. Karczewski, K. J. *et al.* The mutational constraint spectrum quantified from variation in
588 141,456 humans. *Nature* **581**, 434–443 (2020).
- 589 61. Loh, P.-R. *et al.* Efficient Bayesian mixed-model analysis increases association power in
590 large cohorts. *Nat. Genet.* **47**, 284–290 (2015).
- 591 62. Seabold, S. & Perktold, J. Statsmodels: Econometric and Statistical Modeling with
592 Python. *Proceedings of the 9th Python in Science Conference* (2010)
593 doi:10.25080/majora-92bf1922-011.
- 594 63. Ghousaini, M. *et al.* Open Targets Genetics: systematic identification of trait-associated
595 genes using large-scale genetics and functional genomics. *Nucleic Acids Res.* **49**,
596 D1311–D1320 (2021).
- 597 64. Boughton, A. P. *et al.* LocusZoom.js: Interactive and embeddable visualization of
598 genetic association study results. *Bioinformatics* (2021)
599 doi:10.1093/bioinformatics/btab186.
- 600 65. Smith, G. D. & Ebrahim, S. ‘Mendelian randomization’: can genetic epidemiology
601 contribute to understanding environmental determinants of disease? *Int. J. Epidemiol.*
602 **32**, 1–22 (2003).
- 603 66. Slob, E. A. W. & Burgess, S. A comparison of robust Mendelian randomization methods
604 using summary data. *Genet. Epidemiol.* **44**, 313–329 (2020).
- 605 67. Bowden, J. *et al.* A framework for the investigation of pleiotropy in two-sample summary
606 data Mendelian randomization. *Stat. Med.* **36**, 1783–1802 (2017).
- 607 68. Burgess, S., Bowden, J., Fall, T., Ingelsson, E. & Thompson, S. G. Sensitivity Analyses
608 for Robust Causal Inference from Mendelian Randomization Analyses with Multiple
609 Genetic Variants. *Epidemiology* **28**, 30–42 (2017).
- 610 69. Bowden, J., Davey Smith, G. & Burgess, S. Mendelian randomization with invalid
611 instruments: effect estimation and bias detection through Egger regression. *Int. J.*
612 *Epidemiol.* **44**, 512–525 (2015).
- 613 70. Bowden, J., Davey Smith, G., Haycock, P. C. & Burgess, S. Consistent Estimation in
614 Mendelian Randomization with Some Invalid Instruments Using a Weighted Median

- 615 Estimator. *Genet. Epidemiol.* **40**, 304–314 (2016).
- 616 71. Hemani, G., Tilling, K. & Davey Smith, G. Orienting the causal relationship between
617 imprecisely measured traits using GWAS summary data. *PLoS Genet.* **13**, e1007081
618 (2017).
- 619 72. Burgess, S. & Thompson, S. G. Multivariable Mendelian randomization: the use of
620 pleiotropic genetic variants to estimate causal effects. *Am. J. Epidemiol.* **181**, 251–260
621 (2015).
- 622 73. Hemani, G. *et al.* The MR-Base platform supports systematic causal inference across
623 the human phenome. *Elife* **7**, (2018).
- 624